JCSE The Journal of Corrosion Science and Engineering

21st Century Corrosion Science

Volume 6 Paper H057

Metal dusting of iron in CO–H_2–H_2O gas mixtures at 600°C

J. Zhang, A. Schneider, G. Inden

Max-Planck-Institut für Eisenforschung GmbH, Max-Planck-Str. 1, D-40237 Düsseldorf, Germany, j.zhang@mpie.de

Abstract

Iron carburisation and coke formation were investigated at 600°C in (1–95)% CO–(98.8–4.8)% H_2–0.2% H_2O gas mixtures. In all cases, cementite is formed on the sample surfaces together with carbon deposits on the top. With 1% CO, α–Fe particles or an iron layer are formed at the cementite/graphite interface as a result of cementite decomposition. The cementite under this condition vanishes after 21.5 h of reaction. However, for CO contents ≥ 5%, no α–Fe is detected at the interface. The observations of the cross-sections show a very thin cementite layer directly contacted with a thick graphite layer.

Three morphologies of graphite can be identified in the coke of samples carburised by the gas with 1% CO: filamentous carbon, columnar bulk graphite, and graphite particle clusters with many fine iron-containing particles embedded inside. With increasing CO contents, the first two morphologies become the main forms of graphite in the coke. The examination of coke formation in different stages of reaction in the gas with 75% CO shows that the graphite bulks are composed of graphite columns. Filaments develop to the top of surface from the gaps between these columns and distribute preferably along the grinding scratches. Very fine and short filaments are observed in the gases with very low CO content (1–5%) and very high CO content (95%). For CO contents between 5 and 95% long and coarse filaments are observed.

Coke phase analysis by x-ray diffraction reveals that with 1% CO, both iron and cementite are detected. However, above this CO content only cementite is detected as an iron-containing phase in the coke. Thermo-gravimetric analysis shows that the rate of carbon take-up in the early stage of reaction increases with increasing CO content reaching a maximum at 75%.

Keywords: Metal dusting; Carburisation; Cementite decomposition; Coke ; CO content ; Iron particles/layer; Filamentous carbon; Bulk columnar graphite; Graphite particle cluster.

1. Introduction

Metal dusting is a disastrous corrosion phenomenon, degrading iron, low and high alloy steels and Ni- or Co-based alloys in a strongly carburising gas atmosphere (carbon activity $a_C > 1$) at a relatively high temperature (400-800°C). The detrimental consequence of this corrosion includes impairing the heat transfer efficiency, reducing metal catalyst lifetime and damaging the material by separating metal particles to the coke. So far many studies on metal dusting have been published and several mechanisms have been proposed [#ref *1-14*]. Grabke [#ref *1-5*] proposed a mechanism, in which cementite is formed first and then decomposed to fine particles into coke by the initiation of graphite deposition on cementite surface. Recently an extensive study of metal dusting on iron in CO-H_2-H_2O gas mixtures at 700°C was conducted in our laboratory, including the effect of gas composition, cementite decomposition, coke formation, and coke gasification. It was shown that with low CO content α-Fe particles or an iron layer are formed between cementite and graphite [#ref *11-12*]. Increasing the CO content in the gas results in the disappearance of this phenomenon, i.e. cementite contacting directly with the coke layer. Corresponding coke analyses [#ref *13*] indicate the presence of cementite and the absence of iron in the coke if high CO contents are used. Three morphologies of graphite on the surface have been identified as porous graphite clusters, filamentous carbon and bulk dense graphite with a columnar structure [#ref *12*]. The observation of reaction products in different stages of the reaction reveals clearly the process of coke formation. The gasification of carburised samples

provides new information about cementite decomposition in bulk material and in the coke [#ref*14*].

In this work, a comprehensive research work has been conducted on the metal dusting of iron at 600°C which is considered as the worst temperature for metal dusting in CO-H_2-H_2O gas mixtures [#ref*6*]. At this temperature cementite was reported to be decomposed with a fastest rate [#ref*15*]. The aim of this work is to find out whether all phenomena observed at 700°C will also occur at 600°C, e.g. α-Fe layer formation between cementite and graphite etc. The comparison of results at two different temperatures is expected to be helpful to understand the mechanism of metal dusting.

2. Experimental

Pure iron samples (discs of 20 mm in diameter and 1.1 mm in thickness) were used for all metal dusting experiments. The samples were first annealed at 850°C for 1 hour in a pure H_2 gas atmosphere and then ground on SiC paper to grade 1000. Afterwards, the sample was hung on a microbalance (Sartorius 7287 with an accuracy of 1μg) by silica hooks. Helium gas was introduced into the chamber of the microbalance in order to protect the balance. Reaction gases were composed of H_2, CO and H_2O. The content of H_2O was established by passing H_2 through a mixture of oxalic acid and its dihydrate at a certain temperature [#ref*16*]. At first the sample was heated in a pure hydrogen gas atmosphere. After reaching a stable temperature, the reaction gases were introduced into the reactor. The inner diameter of this reactor is 27 mm. The gas compositions were controlled by capillary flow meters. The gas flow rate was fixed at 2 ml/sec. The weight change of the sample during reaction was recorded continuously.

After each carburisation experiment, the quartz filament holding the sample was broken to let the sample drop down into the cold zone for quenching. The surfaces of the samples were analysed by scanning electron microscopy (SEM). After the SEM surface analysis, the specimens were cut to obtain the cross sections for optical microscopy. In order not to alter the surface by the preparation the

samples were coated with nickel and then mounted in epoxy resin. Mounted samples were polished and etched by a hot solution of alkaline sodium picrate for optical microscope observation. In order to detect the phases present in the dust, the coke layer was carefully removed from the surface and analysed by X-ray diffraction (XRD). XRD analysis was performed using monochromatic Co radiation.

3. Results

3.1 Thermogravimetric analysis and cross-section observation

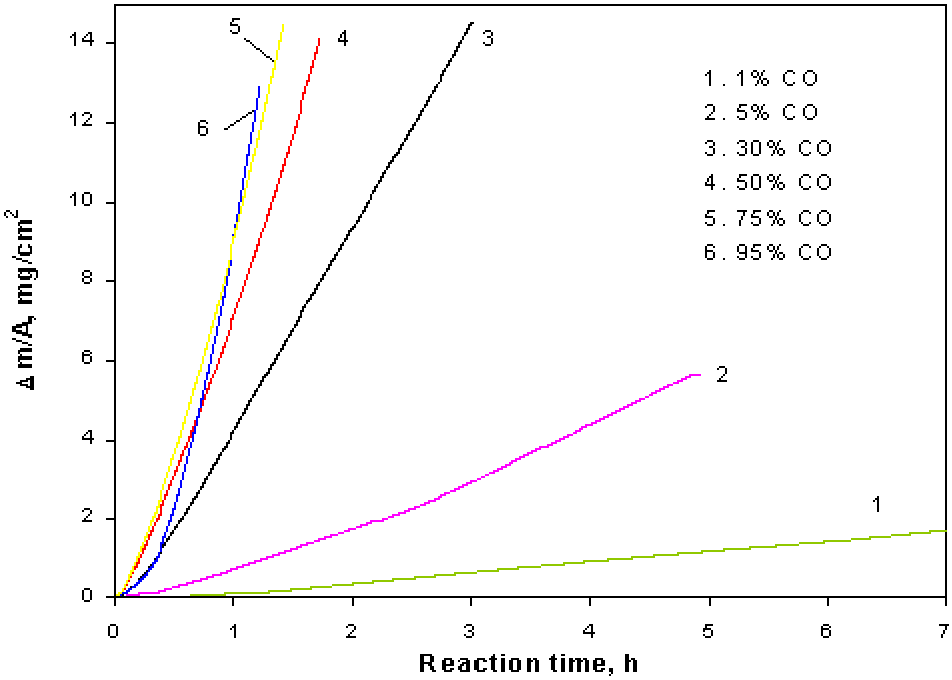

Fig. 1. TGA results of iron samples carburised at 600°C in CO-H_2-H_2O gas mixtures with fixed H_2O content (0.2%) and varied CO contents of (1) 1%, a_c=22.2; (2) 5%, a_c=106.7; (3) 30%, a_c=470; (4) 50%, a_c=559; (5) 75%, a_c=418; and (6) 95%, a_c=102.5.

The effect of gas composition on carburisation of iron was investigated by changing the ratio of H_2 and CO, H_2/CO: (4.8-98.8)/(95-1), but fixing the H_2O content at 0.2%. The corresponding carbon activities [#ref *12*] cover a large area from 22.2 to 559. The weight gains during carburisation are recorded in Fig. 1. All TGA curves can be roughly divided into two parts, corresponding to gradual

increase in the rate of the weight gain at the early stage and to a rapid raise of the rate after a certain time of the reaction. Fig. 1 shows that with increasing CO content the time period of the first stage becomes shorter. The rate of carburisation in the first stage increases with CO contents to the maximum at 75% and then decreases with further increasing CO content to 95%. The rate of carburisation in the second stage keeps its increase with CO contents. Fig. 1 also shows that for CO content higher than 50%, the tendency to increase the rate of carburisation slows down.

Metallographic cross-sections of specimens after different stages of carburisation in 1% CO-98.8% H_2-0.2% H_2O are shown in Fig. 2. After 4.5 h reaction, cementite was formed together with graphite on the top of its surface. Some iron particles are also found between cementite and graphite (Fig. 2a). By increasing the reaction time to 9 h the thickness of graphite and also the amount of iron, which forms even an iron layer between cementite and graphite, are increased (Fig. 2b). After 21.5 h reaction almost all cementite disappears (Fig. 2c).

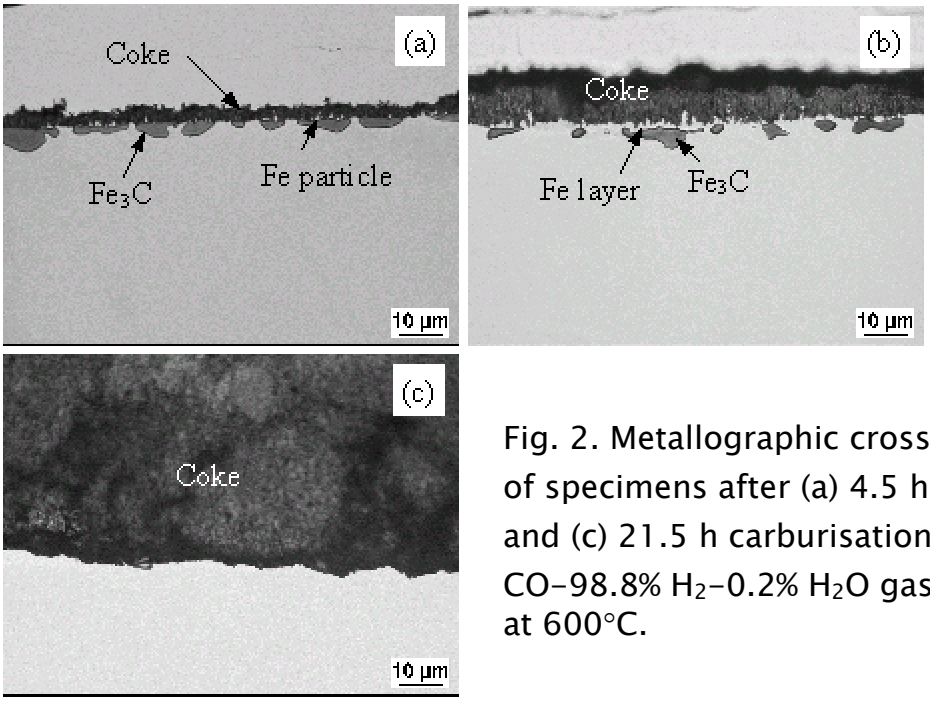

Fig. 2. Metallographic cross-sections of specimens after (a) 4.5 h, (b) 9 h and (c) 21.5 h carburisation in the 1% CO-98.8% H_2-0.2% H_2O gas mixture at 600°C.

This phenomenon, however, does not occur for CO concentrations higher than 5%. The metallographic cross-sections of samples after carburisation by gases with 5-95% CO show a thin cementite and a

thick graphite layer on the top but no iron particles or iron layer between them (Fig. 3b–3f). Fig. 3 also shows that the cementite/graphite interface becomes more serrated by increasing CO contents in the gas. Fig. 3f shows clearly the graphite penetration into cementite layer.

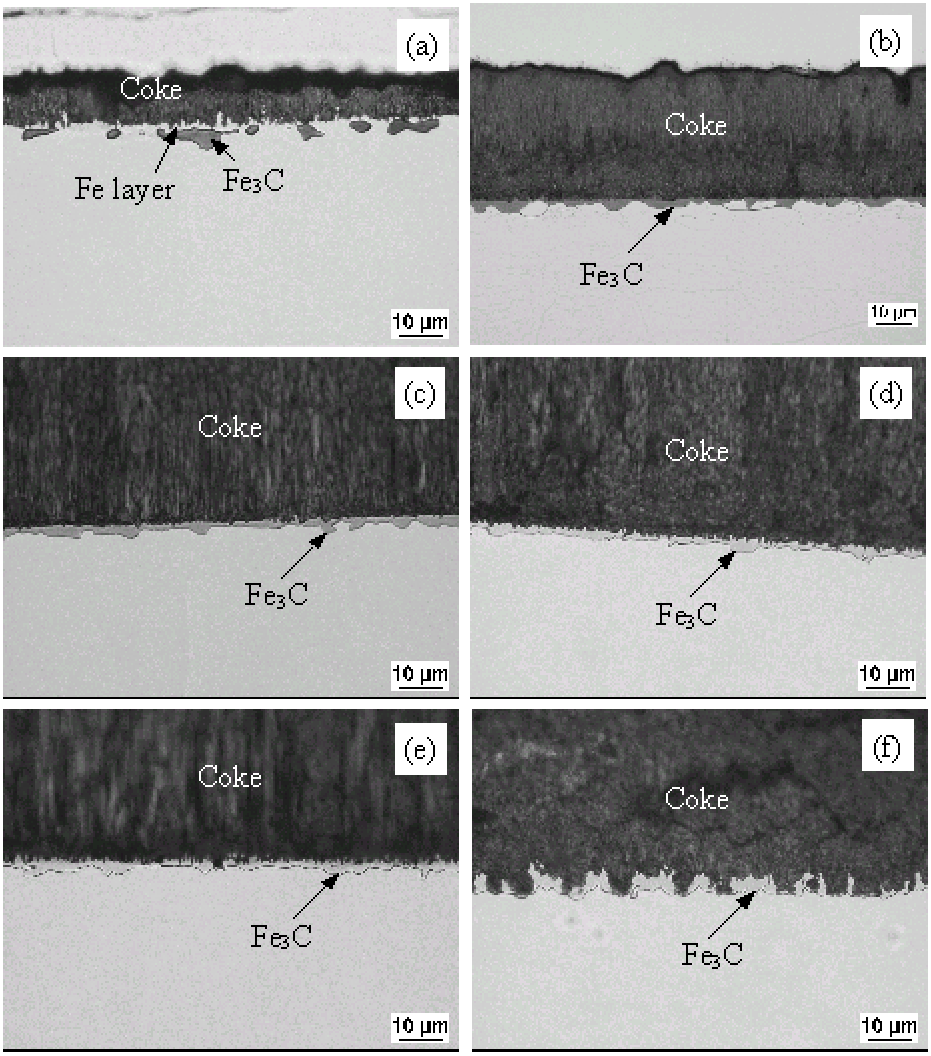

Fig. 3. Metallographic cross-sections of iron samples carburised at 600°C in $CO-H_2-H_2O$ gases (H_2O content fixed at 0.2%) with different CO contents for different reaction times: (a) 1% CO, 9 h; (b) 5% CO, 5 h; (c) 30% CO, 4 h; (d) 50% CO, 2 h; (e) 75% CO, 2 h; and (f) 95% CO, 2 h.

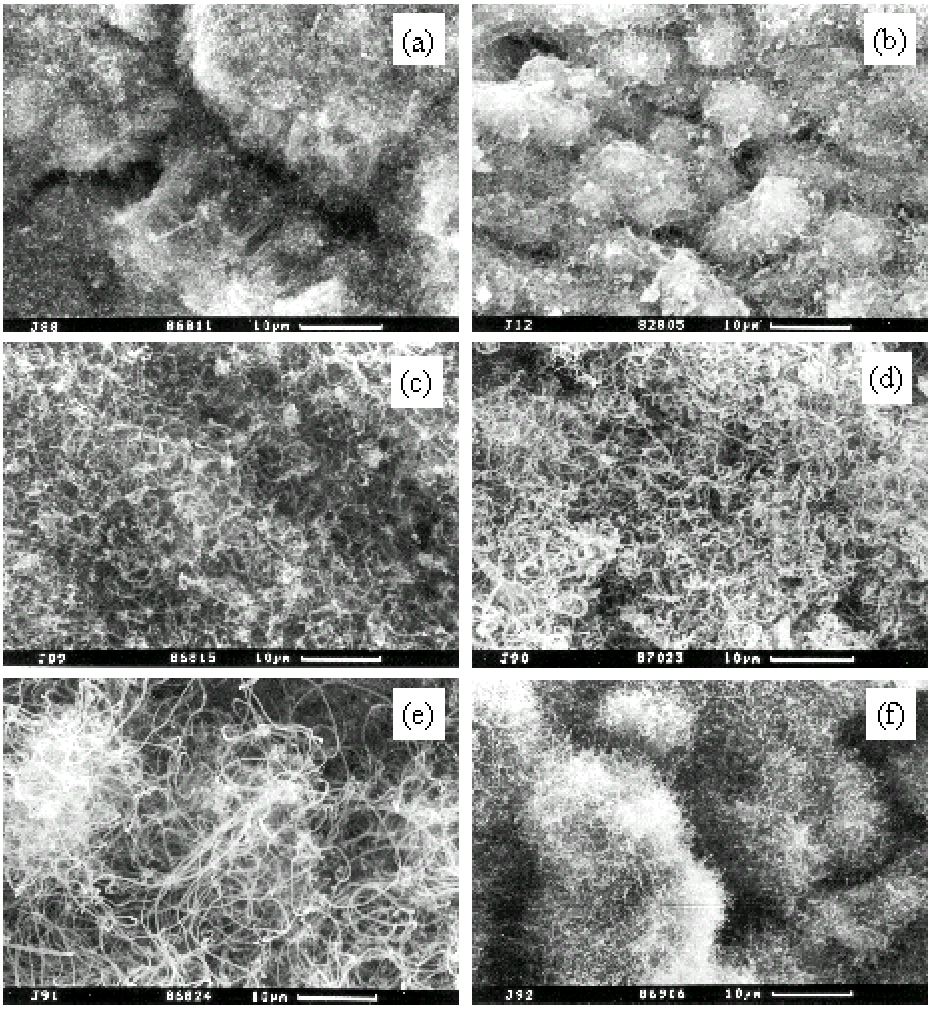

Fig. 4. SEM surface observation of the graphite morphologies of iron samples after carburisation (a) for 21.5 h with 1% CO; (b) for 5 h with 5% CO; (c) for 4 h with 30% CO; and for 2 h with (d) 50% CO; (e) 75% CO and (f) 95% CO in CO-H_2-H_2O gas mixtures (H_2O fixed at 0.2%).

3.2 Surface micro-analysis

Fig. 4 shows the morphologies of graphite on top of the sample surfaces after carburisation with different compositions of the CO-H_2-H_2O gas mixtures. Filamentous carbon is clearly seen in all cases. With low CO contents, e.g. 1 - 5% CO, fine filaments are produced (Fig. 4a-4b). By increasing the CO content to 30% the long and coarse filaments are formed (Fig. 4c). This tendency reaches its maximum when CO content is 75% (Fig. 4e). With further increasing CO content to 95%, the filaments become fine and short again (Fig. 4f).

In the case of low CO contents, especially at 1% CO, very fine filament structures are observed. Therefore, high resolution SEM was used for further analysis. Fig. 5a shows a structure of filaments densely located on the top of a columnar bulk graphite. Fig. 5b gives a high magnification of these filaments. The diameter of these filaments is about 30 nm. In addition to this filamentous carbon, another kind of graphite in the form of particle clusters was also found as shown in Fig. 6. The corresponding back-scatter-electron image of the graphite particle cluster in Fig. 6a shows small metallic particles embedded inside of these graphite particles (Fig. 6b).

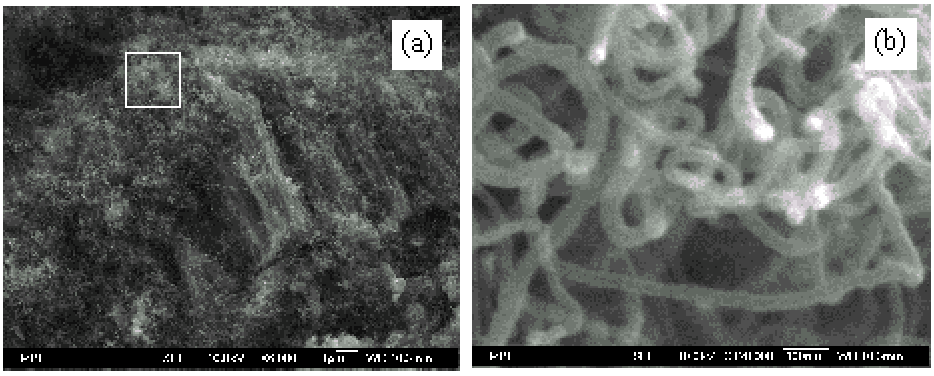

Fig. 5. Morphologies of graphite on the surface of the iron sample carburised at 600°C in the 1% CO-98.8% H_2-0.2% H_2O gas mixture for 21.5 h: (a) low magnification showing very fine filaments and columnar bulk graphite, and (b) high magnification of fine filaments as indicated by the white square in (a).

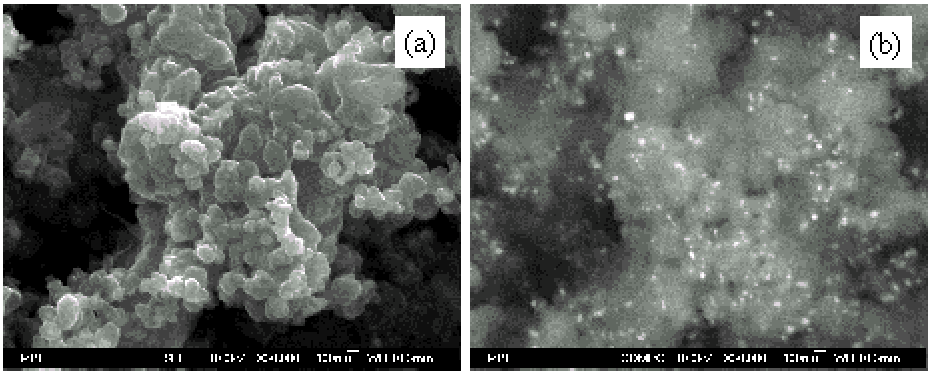

Fig. 6. Graphite with particle cluster structures formed on the surface of the iron sample carburised at 600°C in the 1% CO-98.8% H_2-0.2% H_2O gas mixture for 21.5 h: (a) secondary electron image; (b) corresponding back-scatter electron image.

The structural evolution of carbon deposits on the surface of sample was investigated under the condition of 75% CO-24.8% H_2-0.2% H_2O for 10 min, 0.5 h and 2 h. After 10 min reaction, bulk dense graphite islands are formed on the surface. Some areas of surface are still graphite free as indicated as bright areas in the back-scatter electron image of Fig. 7b. Short filaments are mainly accumulated along grinding scratches (Fig. 7a) and are also bright in back-scatter electron image but with many white points inside (Fig. 7b). After 0.5 h reaction, the whole surface was covered by bulk graphite. Filaments are distributed non-uniformly on the top of bulk graphite and preferably along grinding scratches (Fig. 8a). These graphite bulks seem to be separated from each other, as shown in Fig. 8b. The filaments mainly grow outward from these gaps. By increasing the reaction time up to 2 h, these filaments grow further forming long filamentous carbon clusters (Fig. 8c and 8d).

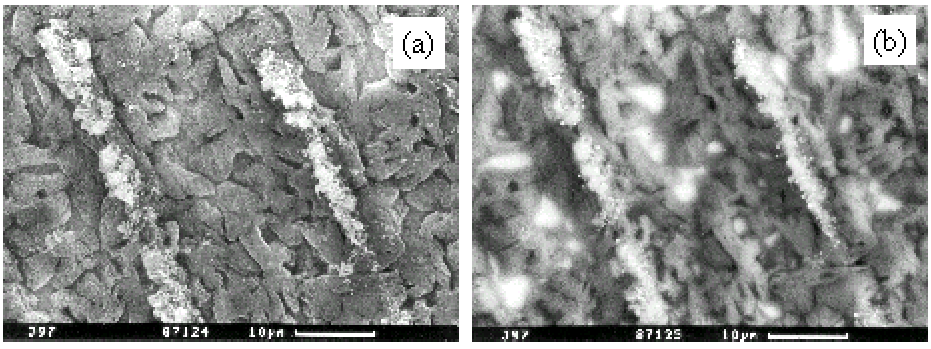

Fig. 7. Carbon deposits on the surface of iron sample after 10 min carburisation in the 75% CO-24.8% H_2-0.2% H_2O gas mixture: (a) a secondary electron image of bulk graphite and filaments along scratches; and (b) the corresponding back-scatter electron image, where bright areas represent filaments and also the surface without carbon coverage.

The different reaction stages in this gas atmosphere (75% CO-24.8% H_2-0.2% H_2O) are characterised by performing optical microscopy of cross-sections, as shown in Fig. 9. Very thin cementite layers are observed in all stages. The thickness of these layers increases slightly with increasing reaction time. The thickness of the graphite on the top of the cementite layer increases remarkably with increasing reaction time. The cross-section of the sample after 2 h carburisation was also analysed by SEM, as presented in Fig. 10. The sample was not polished

after cutting. Figure 10 shows that the bulk graphite layer is composed of many graphite columns. The filaments grow to the top of the surface via the gaps between these columns.

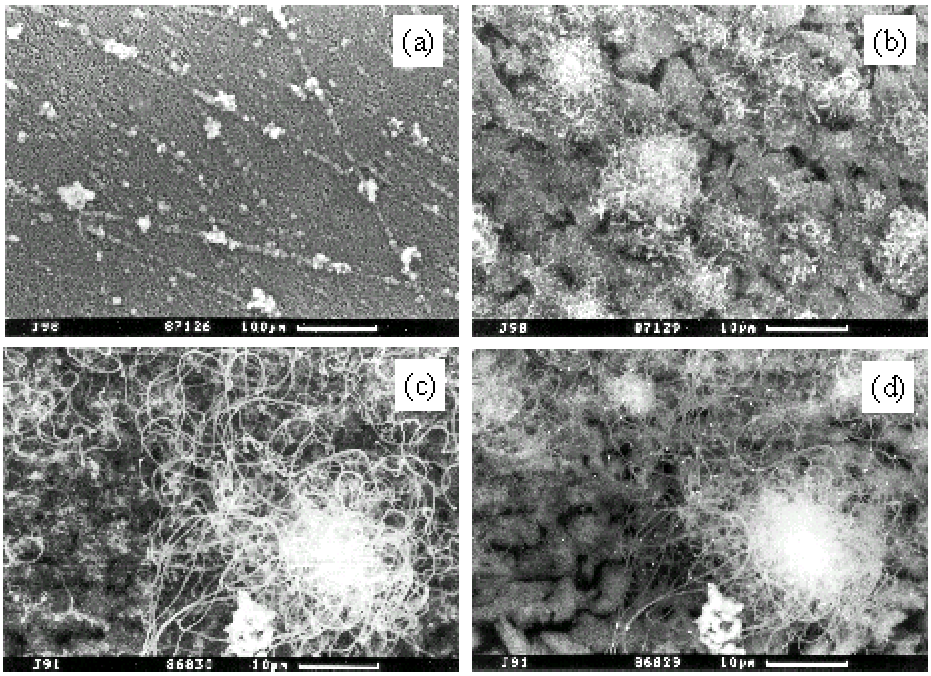

Fig. 8. Carbon deposits on the surface of iron samples carburised in the 75% CO–24.8% H_2–0.2% H_2O gas mixture for 0.5 h in (a) and (b) ((a) low magnification showing bulk graphite and non-uniform filaments; (b) high magnification of this structure); and 2 h in (c) and (d) ((c) secondary electron image and (d) corresponding back-scatter electron image).

3.3 Coke phase analysis

The coke of samples carburised in CO–H_2–H_2O gas mixtures with different compositions was analysed by XRD. The results are shown in Fig. 11. In the case of 1% CO, mainly α-Fe and some Fe_3C are detected, but α-Fe is a main part of iron-containing phase in the coke. However, when the CO contents are above 30%, cementite is the only detectable iron-containing phase in the coke.

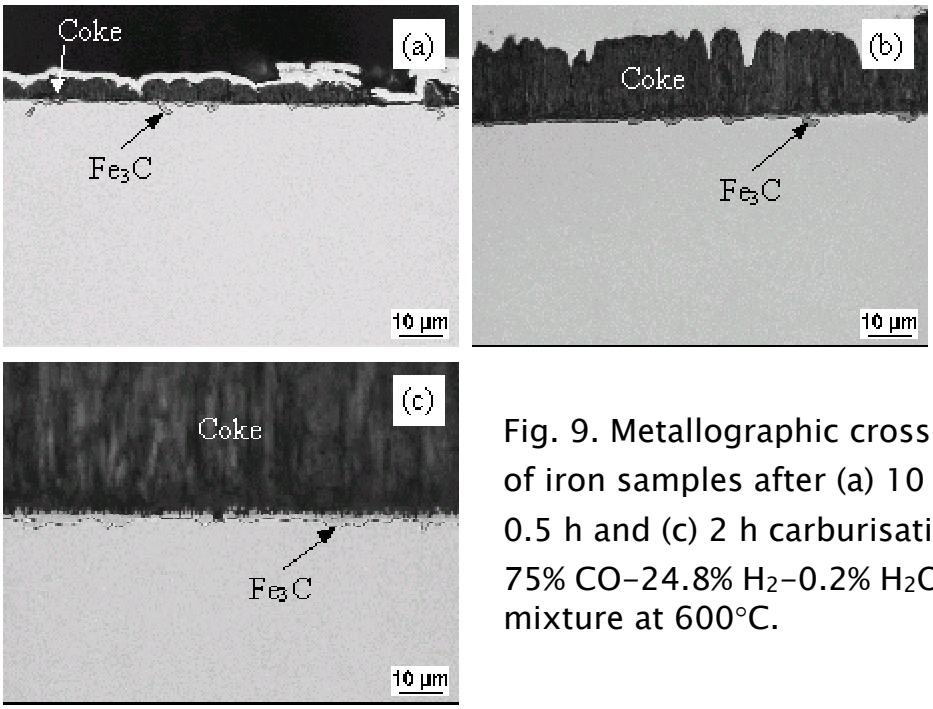

Fig. 9. Metallographic cross-sections of iron samples after (a) 10 min, (b) 0.5 h and (c) 2 h carburisation in the 75% CO-24.8% H_2-0.2% H_2O gas mixture at 600°C.

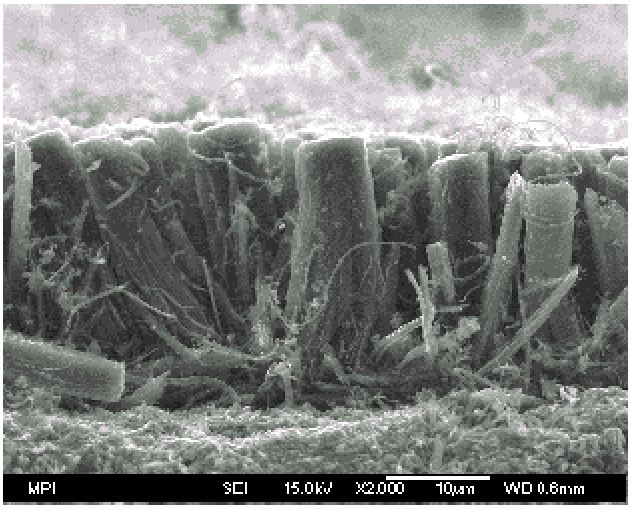

Fig. 10. SEM cross-section observation of the coke layer obtained at 600°C for 2 h in the 75% CO-24.8% H_2-0.2% H_2O gas mixture showing the columnar structure of bulk graphite layer.

4. Discussion

4.1 Iron particles/layer formation between cementite and graphite

The phenomenon of iron particles/layer formation between cementite and graphite was first reported by our past research of metal dusting on iron at 700°C [#ref *11-12*]. At this temperature this phenomenon

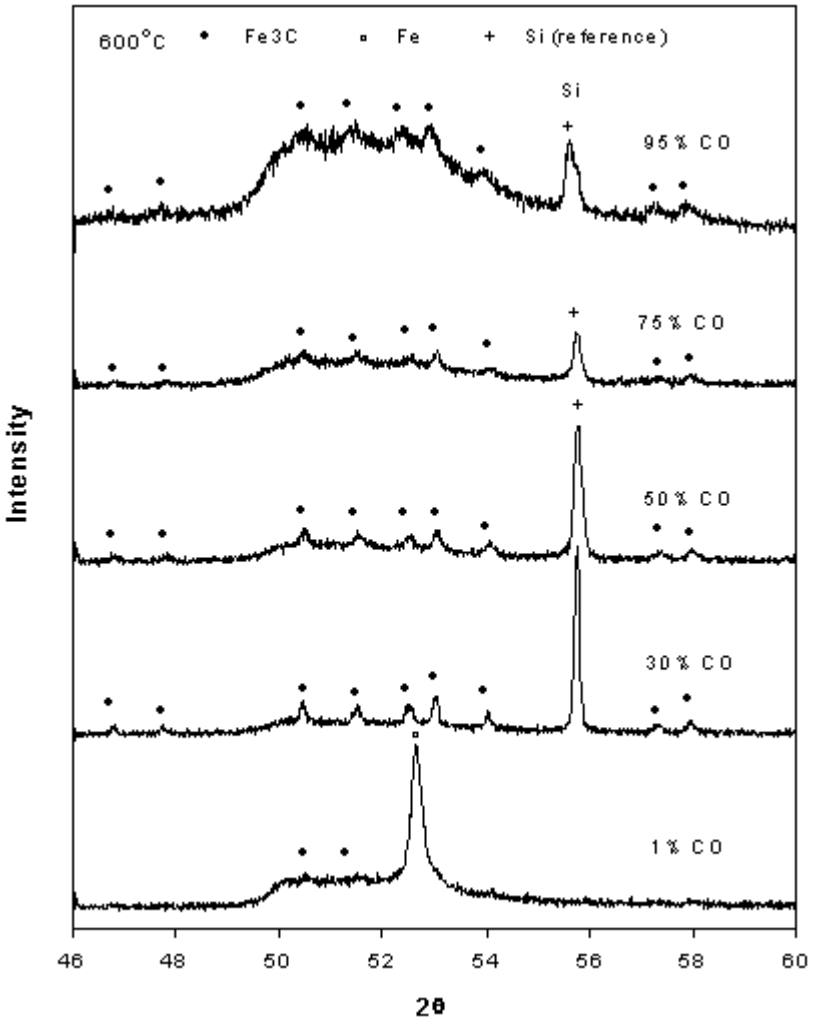

Fig. 11. XRD results of the coke obtained from iron samples carburised in CO–H_2–H_2O (H_2O fixed at 0.2%) gas mixtures for 21.5 h for 1% CO, 4 h for 30% CO and 2 h for 50–95% CO.

appears when CO content is 5% (a_c: 15.8) or below. It was proved that α-Fe at the cementite/graphite interface is a reaction product of cementite decomposition. With a low carbon activity the iron from cementite decomposition accumulates forming iron particles and even a layer between graphite and cementite. It is assumed that the same phenomenon also occurs at other temperatures with a suitable low carbon activity gas. The only expected difference is that the critical content of CO for the formation of this phenomenon differs with temperature. The present results show that this phenomenon occurs when CO content is as low as 1% (a_c: 22.2). It implies that the

occurrence of α-iron layer is determined by the carbon activity of the gas mixture.

4.2 Graphite morphologies

For a low carbon activity gas, e.g. $a_c = 22.2$, three kinds of graphite are observed, very fine filaments with a diameter of about 30 nm, graphite particle clusters with iron-containing particles embedded, and columnar bulk graphite. The formation of fine filaments involves dissolution and diffusion of carbon through the particle [#ref*17*]. Low carbon activity limits this kind of diffusion especially for large particles. The so called graphite particle clusters are very similar to the graphite structure called porous graphite clusters obtained at 700°C with 5% CO [#ref*12*]. Metallic particles are embedded inside of graphite particles, which form a shell structure. These metallic particles are mostly α-Fe as indicated by XRD coke analysis (Fig. 11). It is observed that these iron particles are mechanically detached by inside growth of graphite from the decomposed iron directly contacted with graphite.

By increasing the CO content to above 30% (a_c: 470) only bulk columnar graphite and filaments are observed. The morphology of bulk graphite is different from that at 700°C. In that case bulk graphite is rather dense and cracks are formed by underneath filament growth with subsequent outward growth of filaments [#ref*12*]. However, at 600°C the graphite columns are not closely compact. Carbon filaments can grow outward through the gaps between these columns without breaking the bulk graphite layer.

The formation of filaments was found to have a priority along the grinding scratches. A similar observation was also reported by Schmid et al. [#ref*18*]. It was generally accepted that the deformed area benefits carbon diffusion and graphite nucleation which in turn accelerates the formation of filaments and metal dusting.

4.3 Kinetics of iron carburisation and cementite decomposition

TGA results in this work indicate that the rate of carburisation in the early stage of reaction is increasing with CO content reaching its maximum value at 75% and then decreasing with further increasing CO content. This observation is very similar to the results found at 700°C

[#ref*12*]. In both cases the kinetics of iron carburisation does not reach its maximum at CO and H_2 contents of about 50%. It once again suggests that the rate of carburisation does not fully depend on the reaction of $CO + H_2 = C + H_2O$. The contribution of the reaction $2CO = C + CO_2$ should also be considered especially at high contents of CO [#ref*12*].

The kinetics of cementite decomposition was investigated by Zhang and Ostrovski [#ref*15*] in their study of iron carbide production. They found that cementite produced from iron ore reduction and carburisation by CH_4–H_2 gas decomposes into iron and graphite in both carburisation gas atmosphere and non-carburising atmosphere (Ar gas). They also found that cementite decomposes with a fastest rate at 600°C. By comparing the results in the present work with those at 700°C [#ref*12*], it is found that the rate of cementite decomposition at 600°C is faster than that at 700°C. In the case of iron particles/layer formation between cementite and graphite, after 21.5 h reaction, cementite layer is disappeared completely at 600°C (Fig. 2c), while at 700°C after 20 h reaction, the cementite is still existing but with a decreased amount [#ref*11*]. For the cases without iron particles/iron layer formation, the cross-sections show a very thin cementite layer together with very thick graphite on the top (Fig. 3b–3f). It implies that the decomposition of cementite is very fast at 600°C. The decomposed cementite then catalyses the massive graphite formation. In fact the metal dusting of iron was reported to be the worst at about 575°C by Chun et al. [#ref*6*].

5. Conclusions

Iron carburisation and coke formation were investigated at 600°C in (1–95)% CO–(4.8–98.8)% H_2–0.2% H_2O gas mixtures which cover a large area of carbon activity from 22.2 to 559. In all cases cementite is formed underneath the samples surface together with carbon deposits on its top. Cross-section observations show that with 1% CO, α–Fe particles or a α–Fe layer are formed at cementite/graphite interface. The cementite obtained under this condition evanesces after 21.5 h reaction. The iron particles or iron layers are formed as a reaction product of cementite decomposition. For CO contents larger than 5%,

however, no α-Fe is detected at the interface. The cross-sections in these cases show a very thin cementite layer directly contacted with a thick graphite layer.

The gas composition also affects the morphology of graphite on the surface. In the case of 1% CO, three forms of graphite can be identified in the coke as very fine filamentous carbon, bulk dense graphite with columnar structure and graphite particle clusters with fine iron-containing particles embedded inside. With increasing CO contents, the main forms of graphite are bulk dense graphite and filaments. The examination of coke formation at different reaction stages in a gas mixture with 75% CO reveals the coexistence of bulk graphite columns and carbon filaments. Filaments are preferably located along the grinding scratches and grow outward from the gaps between the graphite columns. Very fine and short filaments are observed in the gases with very low CO content (1-5%) and very high CO content (95%). For CO contents between 5 and 95% long and coarse filaments are observed.

Coke phase analysis by x-ray diffraction reveals that with 1% CO, both iron and cementite are detected. However, only cementite is detected as an iron-containing phase in other gas atmospheres with ≥5% CO. Thermo-gravimetric analysis shows that the rate of iron carburisation in the early stage of reaction increases with increasing CO concentration reaching a maximum at 75%.

Acknowledgements

The authors would like to thank Prof. Grabke for many valuable discussions. The authors would also like to thank Mrs. H. Falkenberg, Mrs. M. Nellessen and Mrs. Angenendt for preparing the metallographic cross-sections and the SEM analysis. Support of this study by the Deutsche Forschungsgemeinschaft is greatly acknowledged.

References

!ref*1* 'On the mechanism of catastrophic carburisation: metal dusting', H. J. Grabke, R. Krajak, J. C. Nava Paz, *Corros. Sci.*, 35, pp1141-1150, 1993.

!ref*2* 'Metal dusting', J. C. Nava Paz, H. J. Grabke, *Oxid. Met.*, 39, pp437-456, 1993.

!ref*3* 'Mechanisms of metal dusting of low and high alloy steels', H. J. Grabke, *Solid State Phen.*, 41, pp3-15, 1995.

!ref*4* 'Carburization and metal dusting on iron', H. J. Grabke, E. M. Müller-Lorenz, A. Schneider, *ISIJ Int.*, 41, Suppl. pp1-8, 2001.

!ref*5* 'Thermodynamics, mechanisms and kinetics of metha dusting', H. J. Grabke, *Mater. Corros*. 49, pp303-308, 1998.

!ref*6* 'Relationship between coking and metal dusting', C. M. Chun, T. A. Ramanarayanan and J. D. Mumford, *Mater. Corros*. 50, pp 634-639, 1999.

!ref*7* 'Micromechanisms of metal dusting on Fe-base and Ni-base alloys', E. Pippel, J. Woltersdorf, R. Schneider, *Mater. Corros.*, 49, pp309-316, 1998.

!ref*8* 'Catastrophic deterioration of high temperature alloys in carbonaceous atmospheres', R. F. Hochman, *Proceedings of the symposium on properties of high temperature alloys with emphasis on environmental effects*, pp 715-732, 1976.

!ref*9* 'Investigation of metal-dusting mechanism in Fe-base alloys using raman spectroscopy, x-ray diffraction, and electron microscopy', Z. Zeng, K. Natesan, V. A. Maroni, *Oxid. Met.*, 58, pp147-170, 2002.

!ref*10* 'Metal dusting of Fe-Cr and Fe-Ni-Cr alloys under cyclic conditions', C. H. Toh, P. R. Munroe, D. J. Young, *Oxid. Met*. 58, pp1-21, 2002.

!ref*11* 'Iron layer formation during cementite decomposition in carburising atmosphere', A. Schneider, *Corros. Sci.*, 44, pp2353-2365, 2002.

!ref *12* 'Effect of gas composition on cementite decomposition and coke formation on iron', J. Zhang, A. Schneider, G. Inden, *Corros. Sci.*, 45 pp281-299, 2003.

!ref *13* 'Characterisation of the coke formed during metal dusting of iron in $CO-H_2-H_2O$ gas mixtures', J. Zhang, A. Schneider, G. Inden, *Corros. Sci.*, 45, pp1329-1341, 2003.

!ref *14* 'Cementite decomposition and coke gasification in He and H_2-He gas mixtures', J. Zhang, A. Schneider, G. Inden, submitted to *Corros. Sci.*.

!ref *15* 'Cementite formation in CH_4-H_2-Ar gas mixture and cementite stability', J. Zhang, O. Ostrovski, *ISIJ Int.*, 41, pp333-339, 2001.

!ref *16* 'The aqueous pressure of some hydrated crystals. Oxalic acid, strontium chloride and sodium sulfate', G. P. Baxter and J. E. Lansing, *J. Am. Chem. Soc*. 42, pp 419-426, 1920.

!ref *17* 'Nucleation and growth of carbon deposits from the nickel catalyzed decomposition of acetylene', R. T. K. Baker, M. A. Barber, P. S. Harris, F. S. Feates, R. J. Waite, *J. Catal.,* 26, pp51-62, 1972.

!ref *18* 'In situ environmental scanning electron microscope observations of catalytic processes encountered in metal dusting corrosion on iron and nickel', B. Schmid, N. Aas, Ø. Grong, R. Ødegård, *Appli. Catal. A: General ,* 215, pp 257-270, 2001.